SUPPORTING INFORMATION

^{17}O solid state NMR as a valuable tool for deciphering reaction mechanisms in mechanochemistry: the case study on the ^{17}O-enrichment of hydrated Ca-pyrophosphate biominerals

Ieva Goldberga,[1,*] Nicholai D. Jensen,[1] Christèle Combes,[2]
Frédéric Mentink-Vigier,[3] Xiaoling Wang,[3] Ivan Hung,[3] Zhehong Gan,[3] Julien Trébosc,[4]
Thomas-Xavier Métro,[5] Christian Bonhomme,[6] Christel Gervais,[6] Danielle Laurencin[1,*]

[1] ICGM, Université de Montpellier, CNRS, ENSCM, Montpellier, France
[2] CIRIMAT, Université de Toulouse, CNRS, Toulouse INP – ENSIACET, Toulouse, France
[3] National High Magnetic Field Laboratory (NHMFL), Tallahassee, Florida, USA
[4] Université de Lille, CNRS, INRAE, Centrale Lille, Université d'Artois FR2638– IMEC– Institut Michel Eugène Chevreul, 59000 Lille, France
[5] IBMM, Université de Montpellier, CNRS, ENSCM, Montpellier, France
[6] LCMCP, UMR 7574, Sorbonne Université, CNRS, Paris, France

*To whom correspondence should be addressed: ieva.goldberga@umontpellier.fr; danielle.laurencin@umontpellier.fr

---

Table of contents

Table S1. 3
Table S2. 3
Figure S1. 4
Figure S2. 4
Figure S3. 5
Figure S4. 6
Figure S5. 6
Figure S6. 7
Figure S7. 7
Figure S8. 8
Figure S9. 9

Table S1. ^{17}O and ^{31}P NMR acquisition parameters of all experiments performed on the *m*-CPPT β and *t*-CPPD samples mentioned in the main text and in the supplementary information (SI) (ν_r – MAS frequency, rd – recycle delay, NS – number of scans).

Figure	Sample	Nucleus	Pulse sequence	^{1}H dec RF / kHz	Field/ T	Rotor Ø/ mm	ν_r / kHz	rd / s	NS
2	*m*-$Ca_2P_2O_7{\cdot}4H_2O$	^{31}P	CP	100	7.0	3.2	8	2	8
2	*m*-$Ca_2P_2O_7{\cdot}4H_2{}^{17}O$	^{31}P	CP	100	7.0	3.2	8	2	8
4		^{17}O	Bloch decay	X	9.4	3.2	18	0.5	35000
4		"	"	X	14.1	3.2	18	0.5	10240
4		"	"	X	18.8	3.2	16	0.5	2048
4 / S3		"	Hahn echo*	X	35.2	3.2	18	0.2	4796
2	*t*-$Ca_2P_2O_7{\cdot}2H_2O$	^{31}P	CP	100	14.1	3.2	8	2	8
2	*t*-$Ca_2P_2O_7{\cdot}2H_2{}^{17}O$	^{31}P	CP	100	14.1	3.2	8	2	8
4		^{17}O	DFS-Onepulse	X	9.4	3.2	18	0.5	80000
4		"	DFS-Onepulse*	100	14.1	3.2	18	0.5	8000
4		"	Bloch decay	X	18.8	3.2	16	0.5	30720
4 / S3			Hahn echo*	X	35.2	3.2	18	0.2	9588

*Phase enriched using 40% ^{17}O-labelled water (90% ^{17}O labelled water for all other samples studied).

Table S2. ^{17}O NMR parameters were calculated for the water molecules using the GIPAW-DFT method. Calculations were performed starting from published crystallographic data, and relaxing H-atom positions (in line with previous experimental-computational studies on these phases).[1]

Phase	Water O Site	δ_{iso} /ppm	C_Q / MHz	η_Q
m-CPPT β	O_{w1}	37.4	8.15	0.88
	O_{w2}	19.7	8.77	0.86
	O_{w3}	19.4	9.45	0.76
	O_{w4}	7.4	8.79	0.85
t-CPPD	O_{w1}	14.5	8.20	0.82
	O_{w2}	22.3	7.70	0.91
m-CPPD	O_{w1}	21.3	9.91	0.72
	O_{w2}	24.0	8.20	0.83

Figure S1. pXRD patterns of the *t*-CPPD phase, before (black) and after (red), ^{17}O enrichment by BM. The pXRD pattern recorded for the *m*-CPPD polymorph is shown in orange, suggesting that traces of this phase may be present in the milled material (blue arrows). This was further confirmed by ^{31}P CP INADEQUATE experiments (Figure S2).

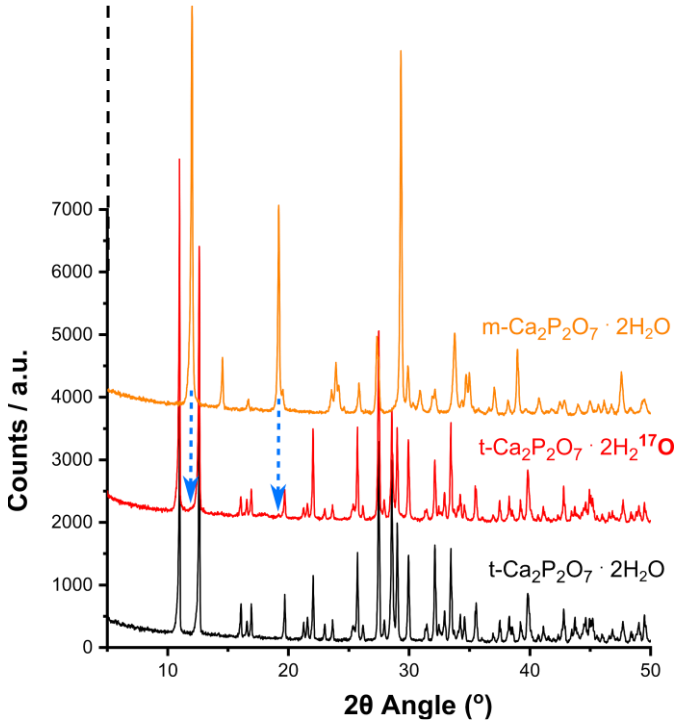

Figure S2. ^{31}P CP-INADEQUATE experiment, recorded on the milled *t*-CPPD phase, showing the presence of the *m*-CPPD form (green-shaded zone). Additional signal intensity around the t-CPPD resonances are caused by partial signal truncation during this experiment and residual dipolar couplings.

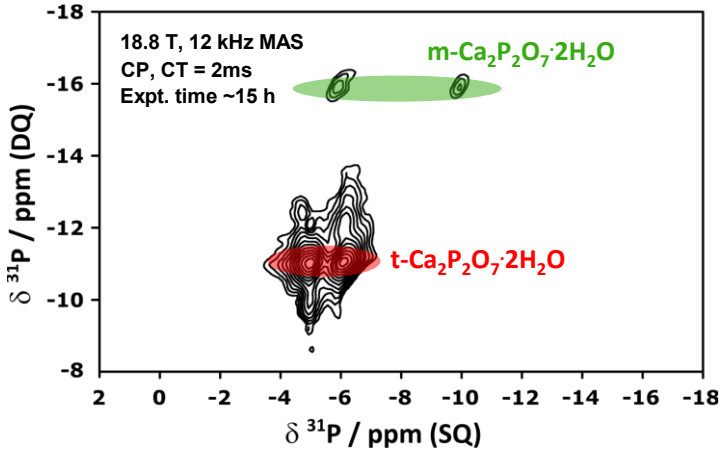

Figure S3. ^{17}O MAS NMR spectra of ^{17}O-enriched *m*-CPPT β and *t*-CPPD, recorded at 35.2 T (zoomed-in version of Figure 4). Acquisition conditions can be found in Table S1. For *m*-CPPT β, the orange arrow points to a high-frequency tailing, which is consistent with the higher-frequency ^{17}O water site calculated by DFT (Table S2, site O_{w1}).

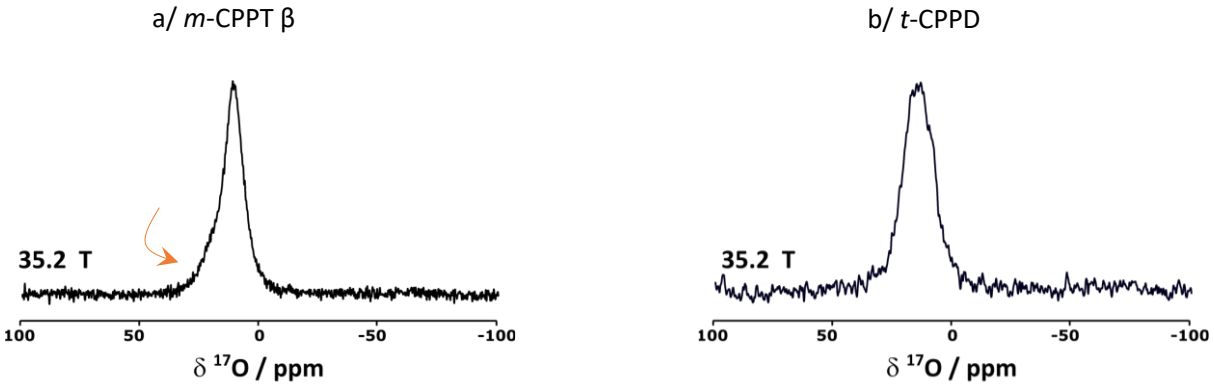

Figure S4. Comparison of the ^{17}O MAS NMR spectrum of the labelled *t*-CPPD phase at 14.1 T, to those simulated from GIPAW-DFT calculations on *t*-CPPD and *m*-CPPD. For the experimental spectrum (in black), acquisition parameters are reported in Table S1. For the calculated spectra, the contributions from the 2 water sites are shown in purple and green dashed lines (see Table S2 for NMR parameters), while the overall spectrum is shown in red. No chemical shift anisotropy was needed in these fits of these MAS spectra, as in our previous studies on COM.[2]

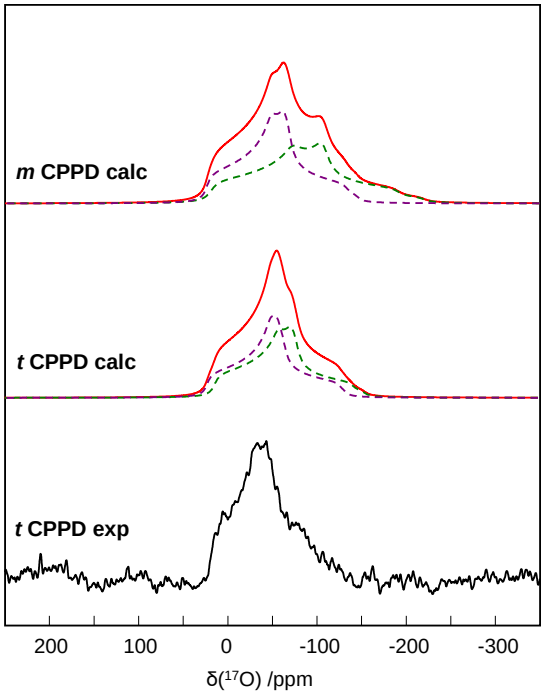

Figure S5. Analysis of the ^{17}O MAS NMR data recorded at multiple magnetic fields for *t*-CPPD (Figure 4, main text), in view of extracting an *averaged* δ_{iso} and P_Q value for the 2 crystallographically inequivalent water molecules.

P_Q is defined as $P_Q = C_Q\sqrt{1+\frac{\eta_Q^2}{3}}$

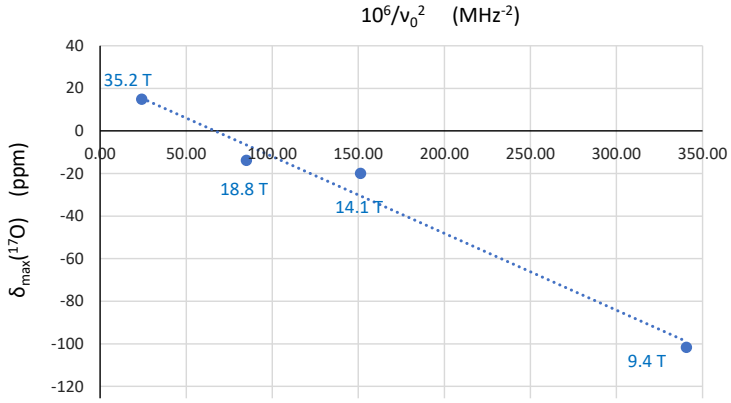

δ_{max} (ppm) = δ_{iso} (ppm) - $\frac{3}{500}\frac{P_Q^2}{\nu_0^2} \times 10^6$

Here, considering the data recorded at 4 different fields:

δ_{max} (ppm) = 24.0 - 0.36 $\frac{10^6}{\nu_0^2}$ (with R^2 = 0.977) → δ_{iso} ≈ 24.0 ppm, and P_Q ≈ 7.7 MHz

Figure S6. Comparison of the ^{17}O MAS NMR spectrum of the labelled *m*-CPPT β phase at 14.1 T, to the one simulated from GIPAW-DFT calculations on *m*-CPPT β. The experimental spectrum is shown in black. For the calculated spectrum, the contributions from the 4 water sites are shown in dashed lines (see Table S2 for NMR parameters), while the overall spectrum is shown in red. No chemical shift anisotropy was needed in these fits of these MAS spectra, as in our previous studies on COM.[2] The experimental spectrum is spread over a much smaller range of chemical shifts than the calculated one, suggesting the presence of dynamics around the water molecules.

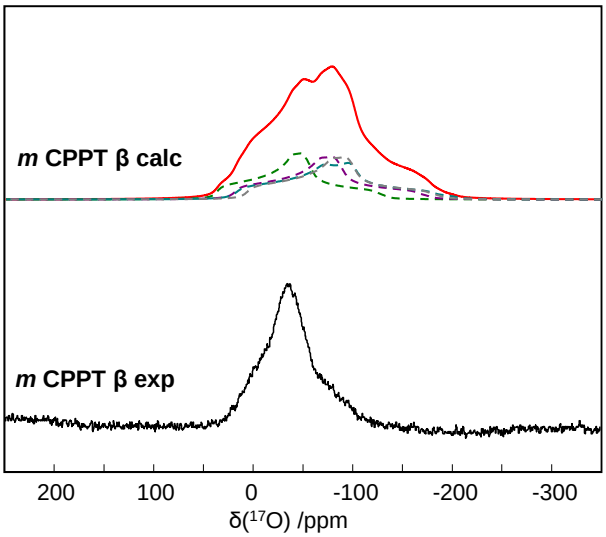

Figure S7. Analysis of the ^{17}O MAS NMR data recorded at multiple magnetic fields for *m*-CPPT β (Figure 4, main text), in view of an *averaged* δ_{iso} and P_Q value for the 4 crystallographically inequivalent water molecules.

P_Q is defined as $P_Q = C_Q\sqrt{1+\frac{\eta_Q^2}{3}}$

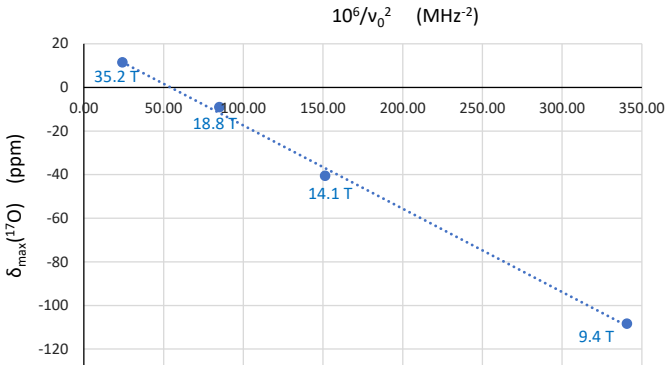

δ_{max} (ppm) = δ_{iso} (ppm) - $\frac{3}{500}\frac{P_Q^2}{\nu_0^2} \times 10^6$

Here, considering the data recorded at 4 different fields:

δ_{max} (ppm) = 20.7 - 0.38 $\frac{10^6}{\nu_0^2}$ (with R^2 = 0.997) → δ_{iso} ≈ 20.7 ppm, and P_Q ≈ 7.9 MHz

Figure S8. ^{17}O solid-state NMR comparison of the labelling level in the *m*-CPPT β and *t*-CPPD phases (at 14.1 T).

a/ Comparison of the ^{17}O MAS NMR spectra of freshly labelled *m*-CPPT β and *t*-CPPD phases, synthesized as described in the experimental section (5 minutes ball-milling at 25 Hz). The initial comparison of spectra is shown on the left, while the display on the right is shown after rescaling for the difference in mass of the sample inside the rotor, and for the difference in weight percentage of water in the two phases is shown on the right. This rescaled data that the enrichment level of water molecules in *m*-CPPT β is ~ 8 times higher than that of *t*-CPPD.

b/ Comparison of the ^{17}O MAS NMR spectra of freshly labelled *m*-CPPT β and *t*-CPPD phases, synthesized as follows: 20 s ball-milling at 25 Hz, followed by 1 night ageing at room temperature in the closed reactor. Essentially no signal was observed in these conditions for the *t*-CPPD phase (even after an overnight acquisition), while a clear signal characteristic of ^{17}O-labeled water was observed in just ~1 hour for *m*-CPPT β. These analyses further prove that *m*-CPPT β is much more straightforward to enrich in ^{17}O, as discussed in the main text.

a/

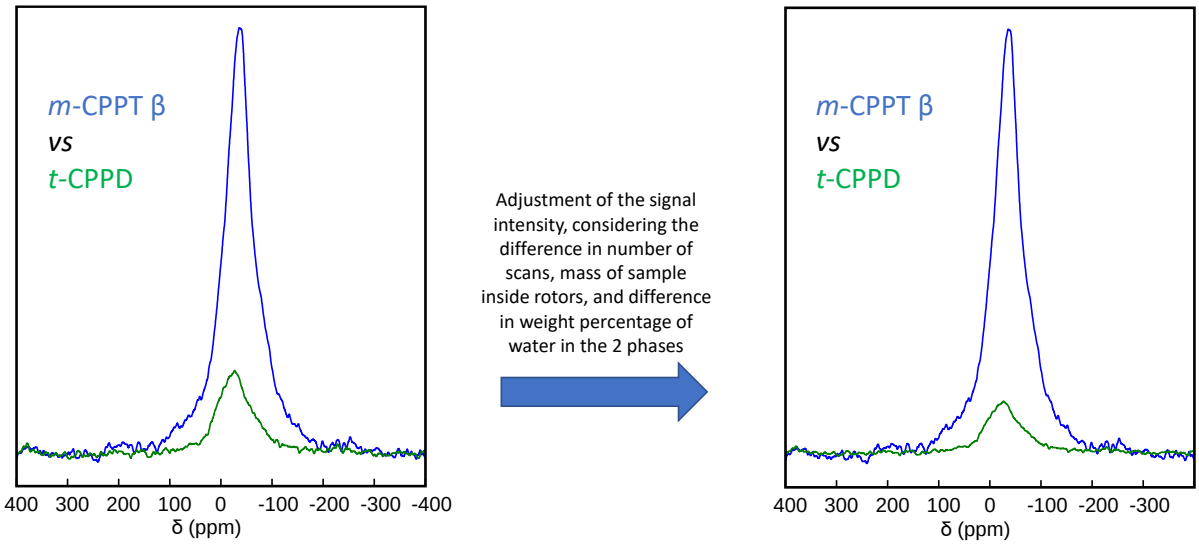

b/

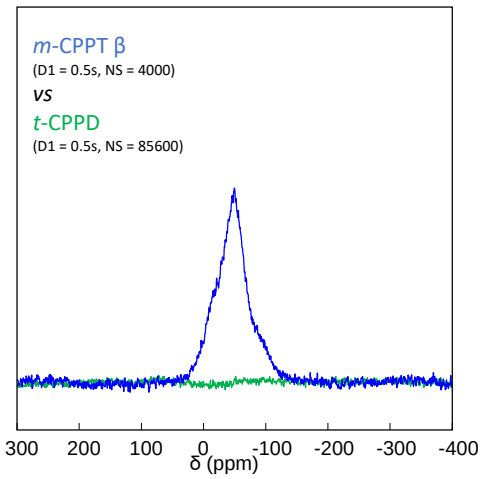

Figure S9. Local environments of the oxygen atoms of the water molecules in *m*-CPPT β and *t*-CPPD. Distances are from the H-relaxed DFT structures used for the GIPAW-DFT calculations (considering here an arbitrary cut-off distance of 2.7 Å).

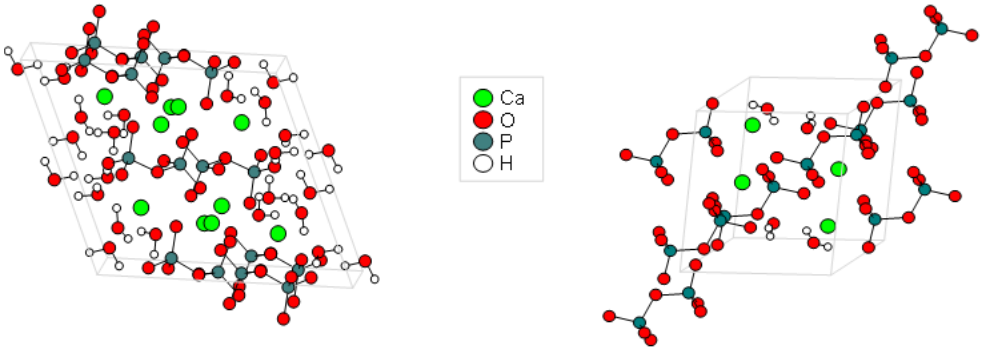

monoclinic $Ca_2P_2O_7.4H_2O$
m-CPPT β

triclinic $Ca_2P_2O_7.2H_2O$
t-CPPD

Water Oxygen	Neighbour	Distance (Å)
O8	H7	0.9824
	H8	0.9998
	Ca1	2.4348
	Ca2	2.5279
O9	H4	0.9805
	H3	0.987
	H7	2.3458
	Ca2	2.4299
	H2	2.4807
	O7	2.6737
O10	H6	0.9774
	H5	0.9872
	Ca2	2.4482
	H7	2.5831
O11	H2	0.9759
	H1	0.9888
	H8	1.7076
	H4	1.9361

Water Oxygen	Neighbour	Distance (Å)
O8	H2	0.9901
	H1	0.9917
	Ca1	2.6092
	Ca2	2.6682
O9	H4	0.9885
	H3	0.9953
	H2	1.9175
	Ca2	2.5268

REFERENCES

[1] Gras, P.; Baker, A. ; Combes, C. ; Rey, C.; Sarda, S. ; Wright, A. J.; Smith, M. E.:; Hanna, J. V.; Gervais, C. ; Laurencin, D.; Bonhomme, C. From crystalline to amorphous calcium pyrophosphates: A solid state Nuclear Magnetic Resonance perspective, *Acta Biomater*. **2016**, *31*, 348-357.

[2] Goldberga, I.; Patris, N.; Chen, C.-H.; Thomassot, E.; Trébosc, J.; Hung, I.; Gan, Z.; Berthomieu, D.; Métro, T.-X.; Bonhomme, C.; Gervais, C.; Laurencin, D. First Direct Insight into the Local Environment and Dynamics of Water Molecules in the Whewellite Mineral Phase: Mechanochemical Isotopic Enrichment and High-Resolution ^{17}O and ^{2}H NMR Analyses. *J. Phys. Chem. C* **2022**. (DOI: 10.1021/acs.jpcc.2c02070)